JOURNAL OF MATERIALS SCIENCE 30 (1995) 3913–3918

# High-$T_c$ superconducting Bi(Al)–Ca–Sr–Cu–O glass-ceramic fibres drawn from glass preforms

YI HU, H. ZHENG, J. D. MACKENZIE
*Department of Materials Science and Engineering, University of California, Los Angeles, CA 90024, USA*

Bi(Al)–Ca–Sr–Cu–O glass-ceramic fibres over 100 cm in length were successfully drawn from a glass preform above the crystallization temperature, $T_x$. The diameters of the uniformly drawn fibres with circular cross-section could be controlled in the range from 25–200 μm and the drawing speed was as high as 200 cm min$^{-1}$. In this work $Al_2O_3$ was used to modify the properties of the glass. It increased the glass transition and crystallization temperatures but did not significantly increase the glass working range. Shrinkage and increase of density during heat treatment of the glass fibres were observed. The annealed (825 °C/12 h in air) $Bi_4Al_{0.1}Ca_3Sr_3Cu_4O_y$ glass-ceramic fibre showed a $T_c$(onset) of 82 K and a $T_c$(zero) of 71 K.

## 1. Introduction

Since the discoveries of high $T_c$ superconducting ceramics, numerous techniques have been adopted or invented to fabricate these materials into the desired forms of fibres or wires [1–5]. For mass production, the glass-ceramic process is one of the promising techniques. One of the advantages of using it for making Bi–Ca–Sr–Cu–O high-$T_c$ superconducting ceramics is the ease of fabricating continuous fibres. In addition, high-density Bi–Ca–Sr–Cu–O superconducting ceramics as well as control of their microstructures can be accomplished by this technique [6–8]. Fibres drawn from Bi–Ca–Sr–Cu–O glass preforms were demonstrated by Onishi *et al.* [4] and Komatsu *et al.* [5]. However, the drawing process was slow and the shape was non-circular. In this work, several issues related to the fast drawing of Bi–Ca–Sr–Cu–O glass fibres from a glass preform were investigated. Bi–Ca–Sr–Cu–O glass fibres were successfully produced by continuous drawing.

It is known that in Bi–Ca–Sr–Cu–O glass crystal growth starts from the surface and grows inwards [9]. Crystallization is influenced by the valence of copper in the glass which is in turn determined by the glass melting condition [10]. Minimization of the devitrification of the glass preform was accomplished by lowering the copper valence of the glasses [10, 11]. Following successful minimization of crystallization of $ZrF_4$-base glasses by doping [12], doping is attempted in this work as an alternative way of avoiding crystallization of the Bi–Ca–Sr–Cu–O glass preforms during fibre-drawing. In Bi–Ca–Sr–Cu–O glass ceramics, the effect of several dopants ($SiO_2$, $B_2O_3$, $GeO_2$, $Al_2O_3$, $Ga_2O_3$, $P_2O_3$) on superconductivity was investigated [13]. It was found that these dopants, except for $Ga_2O_3$, will not destroy superconductivity. The effects of $Al_2O_3$ dopant are investigated here because it was reported that $Al_2O_3$ can stabilize $Bi_2O_3$-based glasses [9], and does not harm superconductivity [14]. It has been found in this work that $Al_2O_3$-doped Bi–Ca–Sr–Cu–O glasses are stable and that continuous glass fibres can be successfully drawn from the glass preforms. The glass fibres were converted into ceramic fibres which exhibit superconductivity with a $T_c$ (onset) of 82 K.

## 2. Experimental procedure

### 2.1. Preparation of glass preform

Regent grade $Bi_2O_3$, $SrCO_3$, $CaCO_3$, CuO and $Al_2O_3$ were used as starting materials and mixed with the nominal composition $Bi_4Al_xCa_3Sr_3Cu_4O_y$ ($x = 0.1$, 0.2, 0.35, 0.5, 0.7, and 1.6). Batches of 15 g of the mixture were melted in a platinum crucible at 1100 °C and poured into a preheated (300 °C) graphite mould, followed by annealing at 300 °C and slow cooling to relieve stresses. Infrared (IR) transmittance analysis was conducted using the KBr pellet method.

### 2.2. Determination of fibre-drawing conditions

Differential scanning calorimetry (DSC) (Perkin–Elmer model DSC-4) was conducted on the glass preforms to determine the glass transition temperature, $T_g$, and crystallization temperature, $T_x$, in air with a heating rate of 10 °C min$^{-1}$.

### 2.3. Processing fibre-drawing

The apparatus is shown in Fig. 1. The glass preform was fixed on a moveable and rotatable drive, and placed in a furnace whose temperature was 20 °C lower than $T_g$ for 10 min to establish thermal equilibrium in the preform. The temperature was then quickly increased to a level temperature at which the

0022–2461

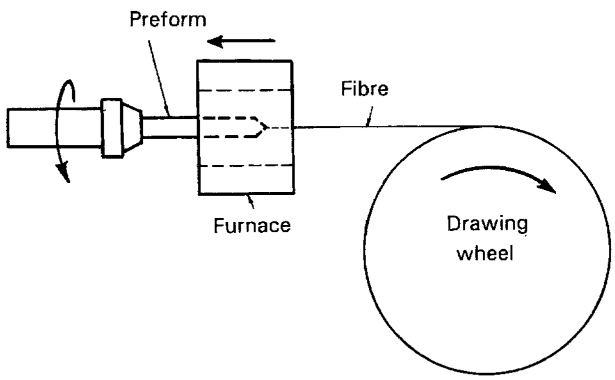

*Figure 1* Preform fibre-drawing apparatus for Bi–Ca–Sr–Cu–O glasses.

glass preform softened and could be drawn into fibres. The diameter of the fibre can be controlled by adjusting the speed of the drawing wheel, the advancing speed of the glass preform and the rotational speed of the preform.

### 2.4. Characterization of preform and fibres

X-ray diffraction (XRD) analysis was conducted on powders of glass and glass-ceramic fibres using Cu$K_\alpha$ radiation, and the microstructure was examined using scanning electron microscopy (SEM). Linear change of the glass preform during the heating process was measured by an Orton automatic recording dilatometer with a heating rate of 3 °C $\text{min}^{-1}$ in air. The density of the fibres was measured by the Archimedes method. Electrical resistivity measurements were made using standard 4-probe d.c. method.

## 3. Results and discussion

### 3.1. Glass formation

As reported, the chosen composition of $Bi_4Ca_3Sr_3Cu_4O_y$ (4334) was much easier to form from the bulk glass than other compositions [14]. The Bi–Ca–Sr–Cu–O glass network is believed to be made up of [$BiO_3$] units which result from the distortion of [$BiO_6$] units by the polarization of heavy metal $Bi^{3+}$ ions [10, 14]. Glass preforms of $Bi_4Ca_3Sr_3Cu_4O_y$ with different $Al_2O_3$ content exhibit the DSC curves in air shown in Fig. 2. It was found that the addition of $Al_2O_3$ can both raise the transition and crystallization temperatures, but does not significantly increase the working range. The rise in $T_g$ is attributed to the presence of $Al_2O_3$ which provides four coordination [$AlO_4$], resulting in a stronger glass network than one with just three coordination [$BiO_3$]. This can be confirmed by the IR spectra shown in Fig. 3. With increasing $Al_2O_3$ the intensity of the characteristic vibration band of [$BiO_3$] at 840 $cm^{-1}$ decreases. In contrast, the absorption peak at 750 $cm^{-1}$, which as reported [9] can be assigned to the stretching vibration of [$AlO_4$] groups, becomes stronger. Alumina (III) doping is anticipated to decrease the polarizing force and thus decrease the number of glass network [$BiO_3$] pyramidal units. Thus, the experimental results indicate that the glass with $Al_2O_3$ addition is easier to make into a preform than one without $Al_2O_3$.

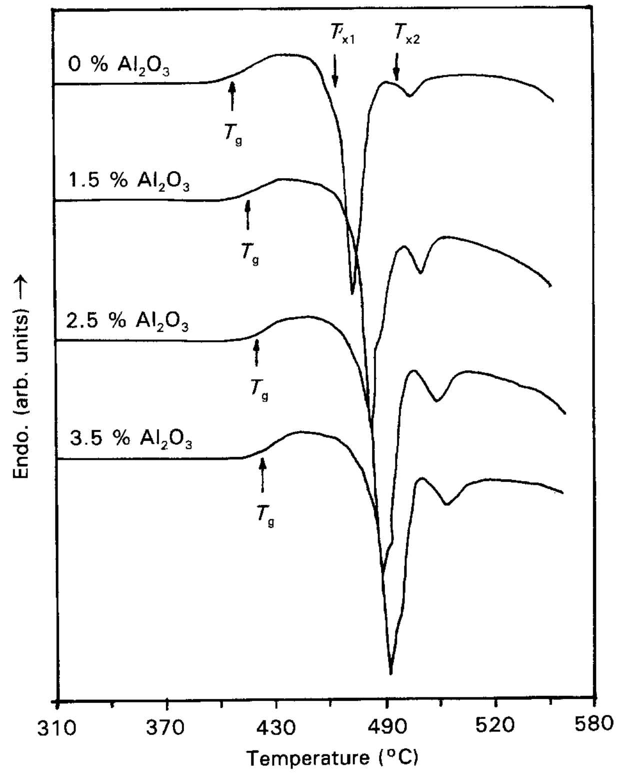

*Figure 2* DSC curves of $Bi_4Ca_3Sr_3Cu_4O_y$ glasses doped with various amounts of $Al_2O_3$.

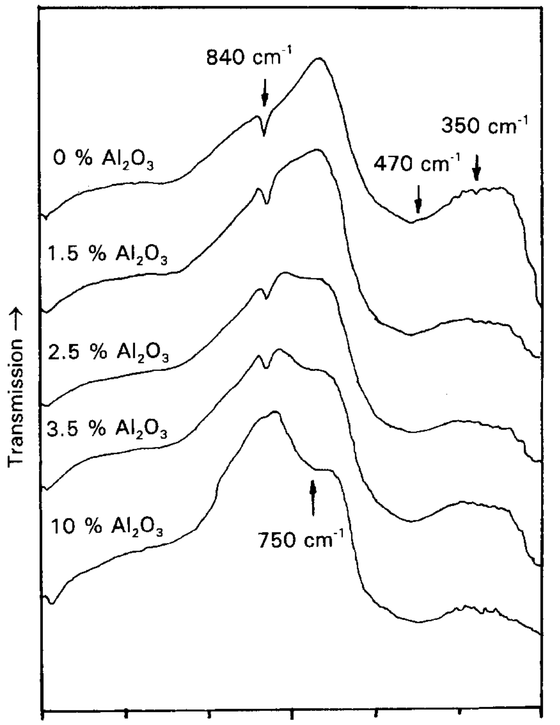

*Figure 3* Infrared spectra of 4334 glass with various $Al_2O_3$ doping.

Compared to $ZrF_4$-based fluoride glasses with the thermal stability range, $\Delta T$ ($T_x - T_g$), of about 100 °C [12], the $\Delta T$ of these $Al_2O_3$-doped bismuth-based

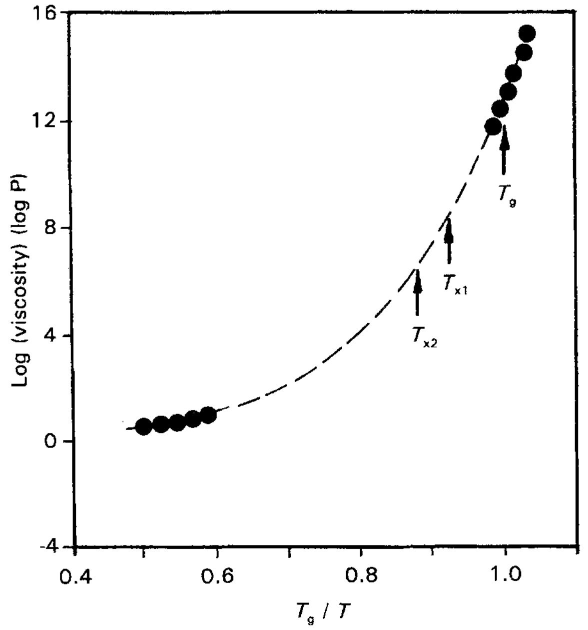

*Figure 4* Viscosity dependence on temperature for $Bi_4Ca_3Sr_3Cu_4O_y$ glasses.

glasses is still narrow. The narrow thermal stability range of bismuth-based glasses would cause great difficulty in fibre-drawing.

## 3.2. Conditions for fibre-drawing

Fibre-drawing from a preform generally is carried out at the glass softening temperature, $T_w$, at which the viscosity of the glass is about $10^{5.5}$ P. Fig. 3 shows the dependence of viscosity on temperature in $Ba_4Ca_3Sr_3Cu_4O_y$ (4334) glasses with non-Arrhenius characteristics [15]. If we want to draw fibre, the temperature as expected should be around or higher than 500 °C as shown in Fig. 4 and will be higher than $T_x$, at which the extrapolated viscosity is still larger than $10^8$ P. Devitrification would then become a problem during fibre-drawing, and that should be avoided or minimized if glass fibres are to be drawn from glass preforms.

Fortunately, the dominant mechanism of crystallization gradually changes from bulk to surface crystallization. It is found that the first crystalline phase of the $Bi_2(Sr,Ca)_2CuO_y$ is formed from the glass [11]. Although the mechanism of crystallization of this glass system at present is not fully clear, previous empirical results, as reported elsewhere [15], imply that it is possible to draw a fibre above the crystallization temperature. If the crystallites initially formed by surface crystallization are very small, they should not stop the movement of the residual glassy phase.

Based on this assumption, the initial crystallite phase size should be estimated. The size of the crystallites on the surfaces of polished specimens with different heating times was observed by SEM, as shown in Fig. 5. It is found that when the crystallite size, $D$, is plotted versus time on a log scale, a straight line is obtained as shown in Fig. 6. The low value of the slope

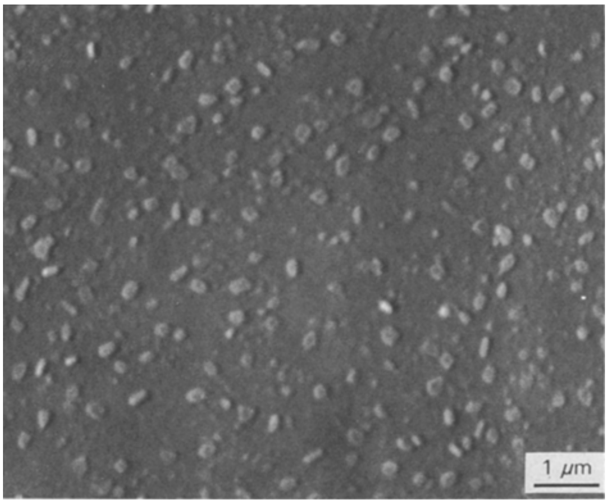

*Figure 5* Crystalline particles on polished glass surface after 12 h heat treatment at 510 °C in air.

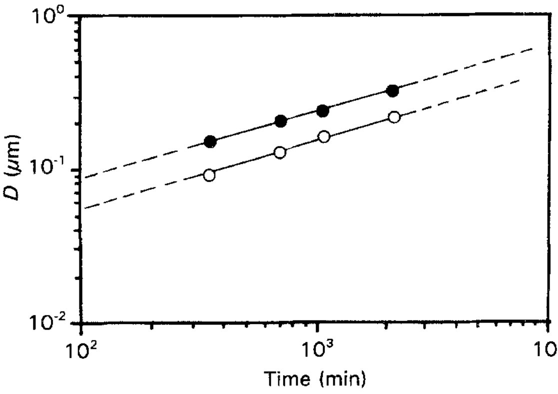

*Figure 6* Size of crystallites on polished glass surface versus heating time at (●) 510 °C, and (○) 460 °C.

( < 0.5 μm $min^{-1}$) indicates that the grain growth rate on the surface of the glass is not high. On the other hand, we did not observe any crystal-like particles inside the samples by SEM until they were heated for a long time, e.g. 520 °C for 48 h. The size of the crystallites in the interior of the sample should be less than 1 nm and is believed to be too small to hinder the motion of residual glasses while drawing fibres.

## 3.3. Fibre drawing

The preform-fibre-drawing apparatus used was described previously (Fig. 1). The drawing zone of the furnace should be properly confined. In the fibre-drawing process, the furnace temperature was first increased to 400 °C and then carefully increased to 480–510 °C where the glass preform softened and could be drawn into fibres. From DSC analysis, the drawing temperature was set at around the onset of the second crystallization temperature ($T_{x2}$). Fibres of over 100 cm were successfully drawn and are flexible as shown in Fig. 7a. The drawing speed was as high as 200 cm $min^{-1}$. Longer fibres could be obtained if the heating zone of the furnace could be confined and the

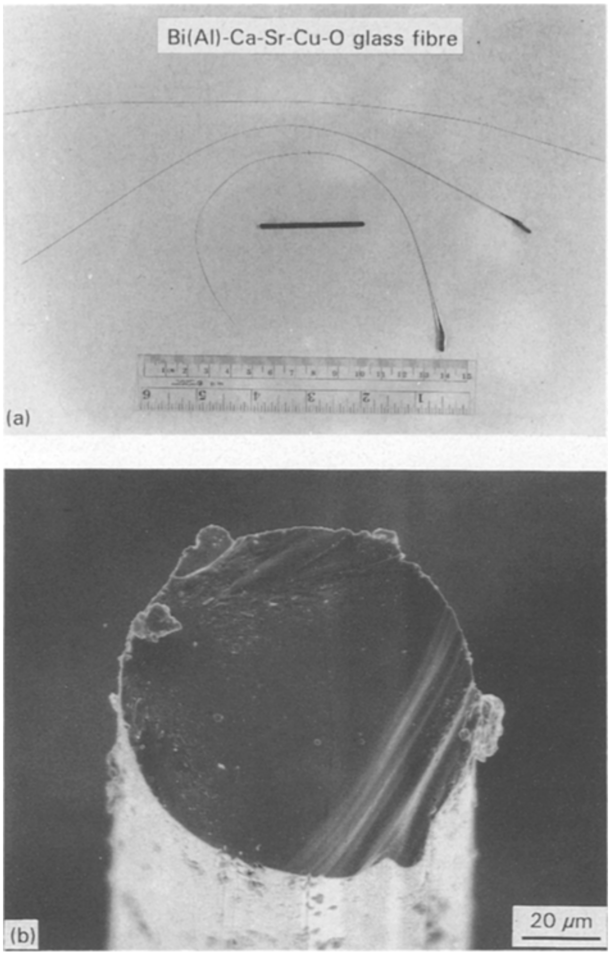

*Figure 7* (a) Different $Al_2O_3$ content doped $Bi_4Ca_3Sr_3Cu_4O_y$ glass fibres and (b) SEM of 1.5 mol % $Al_2O_3$ doped $Bi_4Ca_3Sr_3Cu_4O_y$ glass fibre.

relative feeding rate of the glass preforms could be adjusted properly. The drawn fibres are very uniform, and the shape of the cross-section is circular as shown in Fig. 7b. The diameter of the fibres can be controlled in the range 25–200 μm.

### 3.4. Fibre characteristics

The XRD analysis of the glass preform showed only a very broad peak around $2\theta = 30°$, as shown in Fig. 8. The surfaces and cross-sections of the fibres were investigated by SEM. Very fine particles were found inside the fibres, and there were a large number of spherical crystals with an average size of 0.5 μm on the surface of the fibres, as shown in Fig. 9. The XRD patterns of the drawn fibres (Fig. 8) show a similar glassy state but with an additional halo at around $2\theta = 18°$. This may be caused by local composition variations or initial crystallinity. The crystallites on the surfaces of the fibres were identified by the EDX to be $Bi_2Ca_2CuO_x$, and it has been also confirmed that the glasses first crystallized in the $Bi_2(Sr,Ca)_2CuO_x$ phase at around 500 °C [15].

Crystallite size along the lateral surface of the fibre is very important for the drawing process. Large crystallites will lead to non-homogeneous composition, and a non-uniform and rough fibre surface. The strength of the fibre may also decrease due to many flaws between the particles. Those outer crystalline particles growing faster than those inside the fibre may result from surface crystallization. Oxygen, which can change the copper valence from + 1 to + 2, may be

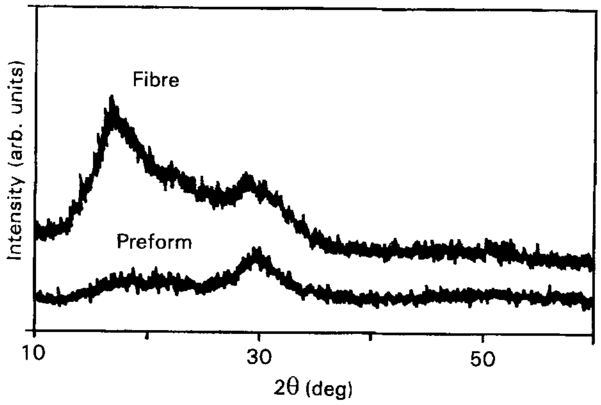

*Figure 8* X-ray diffraction patterns of $Bi_4Al_{0.2}Ca_3Sr_3Cu_4O_y$ glass preform and drawn fibres.

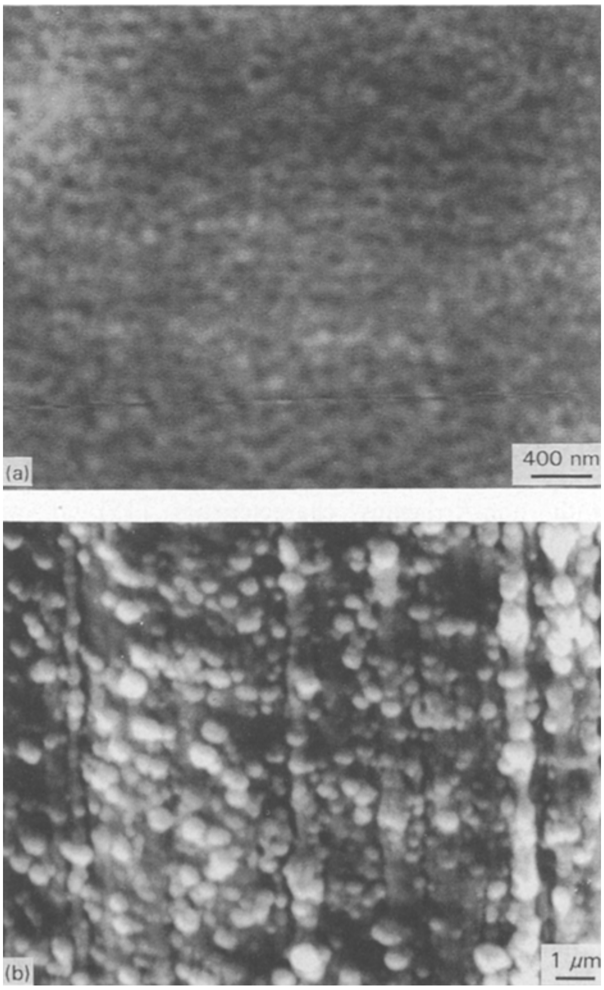

*Figure 9* Scanning electron micrographs of (a) the interior area and (b) drawn fibre surface with 1.5 mol % $Al_2O_3$.

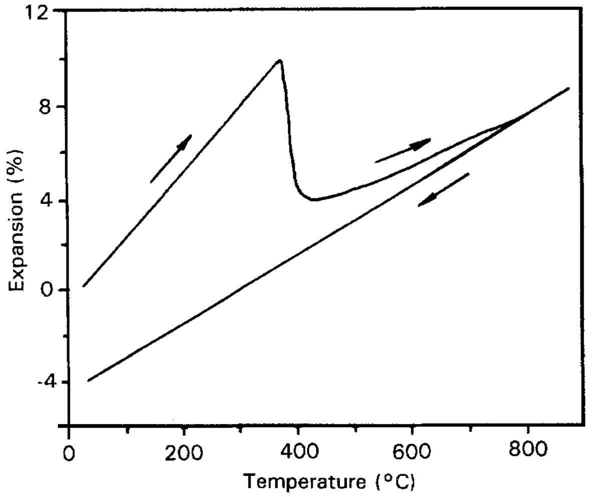

*Figure 10* Longitudinal shrinkage percentage and the density variation versus heat treatment in 1 h.

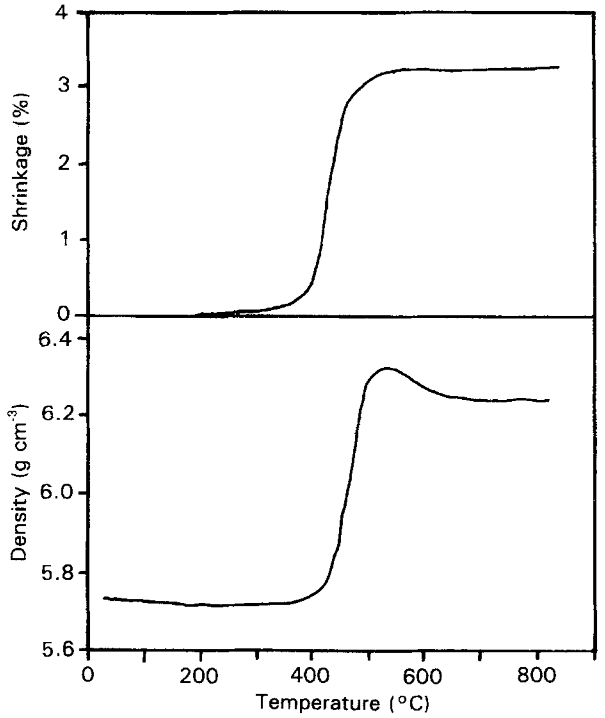

*Figure 11* Linear changes of 2.5 mol % $Al_2O_3$ doped $Bi_4Ca_3Sr_3Cu_4O_y$ glass during heating process.

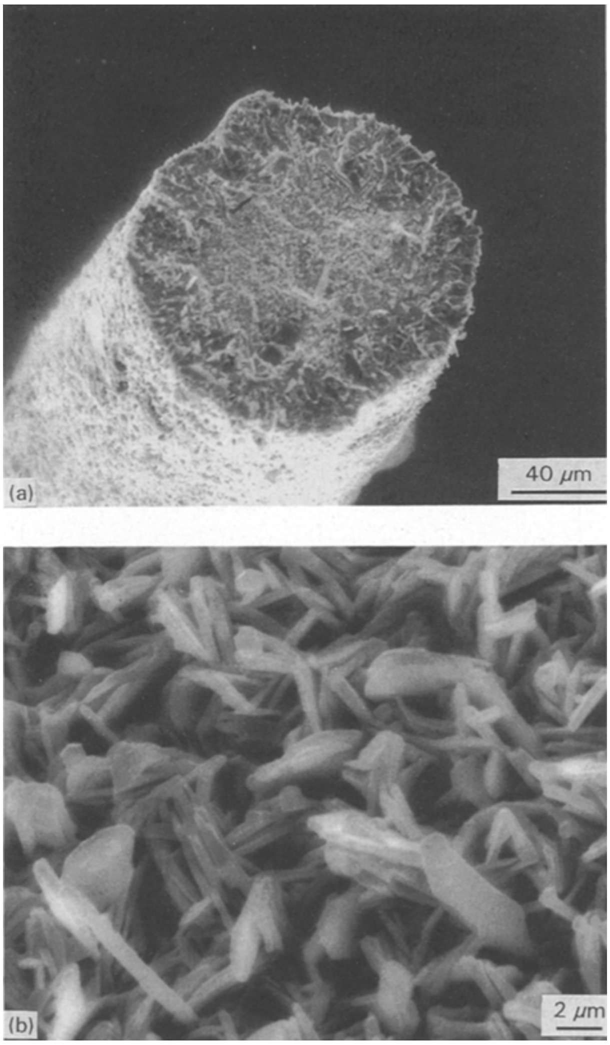

*Figure 12* Scanning electron micrographs of (a) the interior area and (b) the drawn fibre surface with 2.5 mol % $Al_2O_3$ doped in $Bi_4Ca_3Sr_3Cu_4O_y$ glass after 12 h treatment at 825 °C in air.

the main factor in enhancing the growth of (2 0 2 1) phase. Mechanical polishing or chemical etching processes on preform that have been successfully applied to fluoride glass optical fibres are suggested before fibre-drawing [16].

Fig. 10 shows the shrinkage in longitudinal direction and the density of the fibres as a function of heat-treatment temperature for 1 h. Most shrinkages and the density variations, which are due to the relaxation and crystallization of the glasses, occurred from 350–500 °C. The linear change in the glass preform versus heating process is shown in Fig. 11. The expansion coefficient of glass, $1.32 \times 10^{-5}\,°C^{-1}$, is much higher than that of the ceramic, $7 \times 10^{-6}\,°C^{-1}$. It is very important to control fibre shrinkage and expansion during heat treatment for obtaining superconductivity to avoid fibre distortion.

The microstructure of the fibres after heat-treatment is shown in Fig. 12a. The surface of the fibre shown in Fig. 12b has the common plate characteristics of the superconducting phase. Fig. 13 shows the XRD pattern of the fibres fired at 825 °C for 12 h in air followed by furnace cooling. It has been found that even samples with 10 mol %$Al_2O_3$ still have the main phase of $Bi_2CaSr_2Cu_2O_y$ (2 1 2 2). It has also been confirmed that aluminium plays an insignificant role in superconductivity but that it can change the processing conditions [17]. Fig. 14 shows the temperature dependence of resistivity for heat-treated fibres with different amounts of $Al_2O_3$ doping. The 4334 glass-ceramic sample with $x = 0.1$ of $Al_2O_3$ shows $T_c$ (onset) at about 82 K and a $T_c$ (zero) at about 71 K. Samples with a larger addition of $Al_2O_3$ show higher resistivity above the onset temperature. $Al_2O_3$ may act as an impediment to electrical conducting or a second phase to hinder complete crystallization of the superconducting phase.

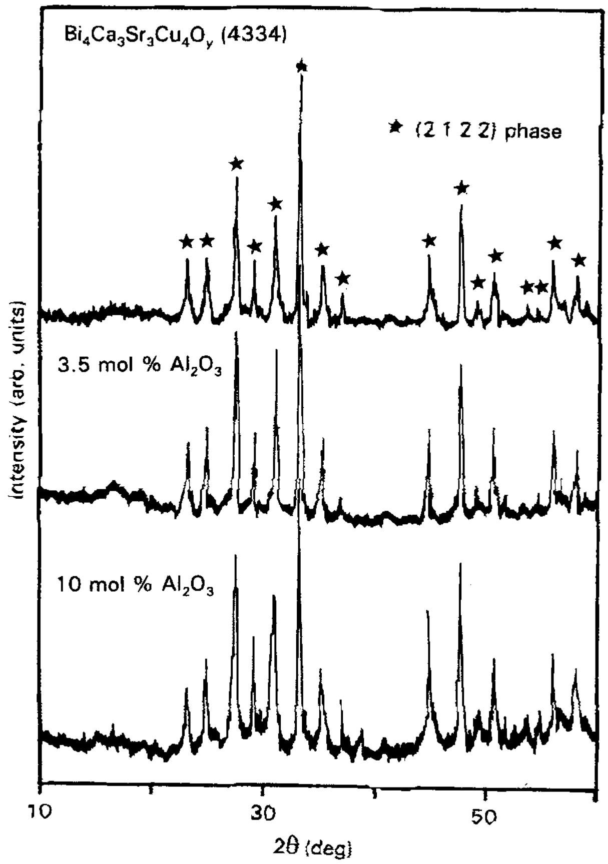

*Figure 13* X-ray diffraction patterns of various $Al_2O_3$ content-doped $Bi_4Ca_3Sr_3Cu_4O_y$ fibres after 12 h heat treatment at 825 °C in air.

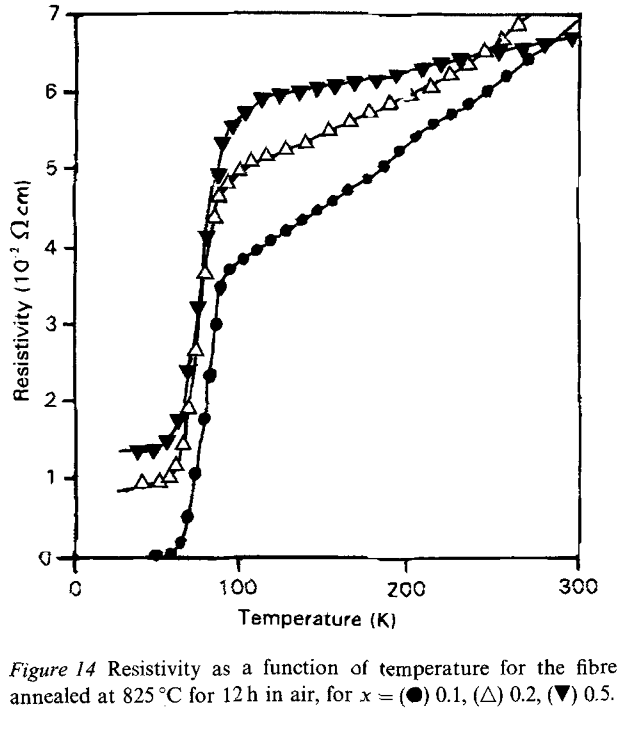

*Figure 14* Resistivity as a function of temperature for the fibre annealed at 825 °C for 12 h in air, for $x$ = (●) 0.1, (△) 0.2, (▼) 0.5.

## 5. Conclusion

Bi(Al)–Ca–Sr–Cu–O fibres more than 100 cm long have been successfully fabricated by the glass-preform fibre-drawing technique at a temperature higher than the crystallization temperature, $T_x$. The diameters of the drawn fibres can be controlled in the range 25–200 μm. Devitrification problems do not seriously affect the fibre drawing process because the small crystallites do not hinder the movement of the residual glass. The addition of $Al_2O_3$ can aid glass forming and make fibre drawing easier, although there is no large increase in the extension of the working range. The thermal properties of the drawn fibres show shrinkage and extension problems during heating. The fibre with 1.5 mol % $Al_2O_3$ annealed at 825 °C for 12 h in air exhibits $T_c$ (onset) at 82 K and $T_c$ (zero) at 71 K.

## Acknowledgements

This work was supported by the Strategic Defense Initiative and the Air Force Office of Scientific Research, Directorate of Chemical and Atmospheric Science.

## References

1. G. F. DELAFUENTE, R. NAVARRO, F. LERA and C. RILLO, *J. Mater. Res.* **6** (1991) 699.
2. A. KUROSAKA, M. AOYAGI, H. TOMINAGA, O. FUKUDA and H. OSANAI, *Appl. Phys. Lett.* **55** (1989) 390.
3. S. KATAYAMA and M. SEKINE, *J. Mater. Res.* **6** (1991) 1629.
4. M. ONISHI, T. KOHGO, Y. CHIGUSA, K. WATANABE, M. KYOTO and M. WATANABE, *Jpn J. Appl. Phys.* **29** (1990) L64-L66.
5. T. KOMATSU, C. HIROSE, T. OHKI, R. SATO and K. MATUSITA, *Appl. Phys. Lett.* **57** (1990) 183.
6. H. ZHENG and J. D. MACKENZIE, *Phys. Rev. B* **38** (1989) 7166.
7. T. KANAI, T. KUMAGAI, A. SOETA, T. SUZUKI, K. AIHARA, T. KAMO and S. MATSUDA, *Jpn J. Appl. Phys.* **27** (1988) L1435.
8. N. TOHGE, S. TSUBOI, Y. AKAMATSU, M. TATSUMISAGO and T. MINAMI, *Nippon Seramikkusu Kyokai Ronbunshi* **97** (1989) 334.
9. R. XU, H. ZHENG and J. D. MACKENZIE, in "Superconductivity and Ceramic Superconductors", edited by K. M. Nair and E. A. Giess (American Ceramic Society, Westerville, OH, 1990) pp. 653–67.
10. H. ZHENG, M. W. COLBY and J. D. MACKENZIE, *J. Non-Cryst. Sol.* **27** (1991) 143.
11. H. ZHENG and J. D. MACKENZIE, *Phys. Rev. B* **43** (1991) 3048.
12. D. C. TRAN, R. J. GINTHER and G. H. SIGEL Jr, *Mater. Res. Bull.* **17** (1982) 1177.
13. H. ZHENG and J. D. MACKENZIE, in "Proceedings of the XV International Congress on Glass", USSR, 1989, to be published.
14. H. ZHENG, R. XU and J. D. MACKENZIE, *J. Mater. Res.* **4** (1989) 911.
15. H. ZHENG, Y. HU and J. D. MACKENZIE, *Appl. Phys. Lett.* **58** (1991) 1679.
16. H. W. SCHNEIDER, A. SCHOBERTH and A. STANDT, *Glastech. Ber.* **60** (1987) 205.
17. C. W. CHU, J. BECHTOLD, L. GAO, P. H. HOR, Z. J. HUANG, R. L. MENG, Y. Y. SUN, Y. Q. WANG and Y. Y. XUE, *Phys. Rev. Lett.* **60** (1988) 941.

*Received 6 May 1993*
*and accepted 9 June 1994*